# VERIFICATION AND OPTIMIZATION OF VDES BY COUPLING THE FREE-BOUNDARY EQUILIBRIUM AND TRANSPORT CODES WITH CONTROL IN THE HL-3 TOKAMAK

EX-S

***Experimental validation of $FF+FB$ control strategy based on a non-linear plasma model***


X. Song, L. Xue, Y.H. Cheng, J.Z. Zhang, T.F. Sun, Y.H. Zhang, Y.Y. Zhong, D. Li, P.L. Liu, L. Liu, J.X. Li, S. Wang, H.L. Du, M. Xue, G.Y. Zheng, W.L. Zhong

Southwestern Institute of Physics, Chengdu, 610041, China

E-mail: songx@swip.ac.cn


Vertical displacement events (VDEs) [1] are one of the main causes of major disruption that could damage plasma facing components, especially in reactor-size tokamaks. For example, only two major disruptions are allowed throughout all stages of ITER operation. Elongated plasma, an effective approach to enable high plasma confinement, is inherently vertically unstable. Additionally, perturbations in other parameters, such as poloidal beta $\beta_p$, internal inductance $l_i$ and toroidal current density $j_\phi$, can also increase the vertical growth rate of VDEs, making it very difficult to precisely control the plasma vertical position. Therefore, it is a high priority to evaluate VDEs in closed-loop simulation with high-fidelity models.

In this work, an integrated workflow is developed to verify and optimize VDE predictions in the HL-3 tokamak. A simple schematic is shown in Fig. 1. The workflow is divided into two parts, i.e. plasma control and the non-linear plasma model. The plasma model is designed to replace the plasma evolution when there is no discharge commissioning, while the plasma control loop remains the same as the one embedded in the PCS. The objective of feedback ($FB$) control is $R$, $Z$ and $I_p$, with the control strategy based on coil voltages. Notably, coil currents are not explicitly involved in the $FB$ loop [2]. The reference trajectories for $R$, $Z$, $I_p$ and coil voltages ($V_{PF}$) in feedforward ($FF$) settings are determined through optimizations or trail and error by pilots. The gains in the PID controller are also aligned with the PCS. At the core of the workflow is a non-linear plasma mode, which is numerically coupled using the free-boundary equilibrium code FEEQS.M [3] and the fast transport code METIS [4]. In FEEQS.M, the circuit equations for the PF coil system are coupled with the G-S equation to compute the evolution of $(R,Z)$, elongation ($\kappa$) and ($\delta$), using the input $V_{PF}^{FF}+V_{PF}^{FB}$ from the plasma control loop. The evolution of $I_p$ depends on the plasma self inductance ($L_p$), resistance $R_p$, loop voltages ($V_{loop}$) and non-inductive $I_p^{ni}$. Based on the FEEQS.M results, $L_p$ and $V_{loop}$ , which is derived from the time derivative of magnetic flux at plasma boundary $\psi_{bnd}$, are determined. With input experimental data, such as line-averaged density ($\overline{n_e}$), effective atom number ($Z_{eff}$) and auxiliary heating power ($P_{aux}$), METIS calculates $R_p$ (Spitzer model) and $I_p^{ni}$ (includes bootstrap, runaway and auxiliary heating currents) based on scaling laws. Moreover, parameters are exchanged between FEEQS.M and METIS, i.e. FEEQS.M retrieves $\beta_p$, $l_i$ and/or $j_\phi$ from METIS, while passing to METIS with plasma shape parameters, including major radius ($R_0$), minor radius ($a$), $\kappa$ and $\delta$.

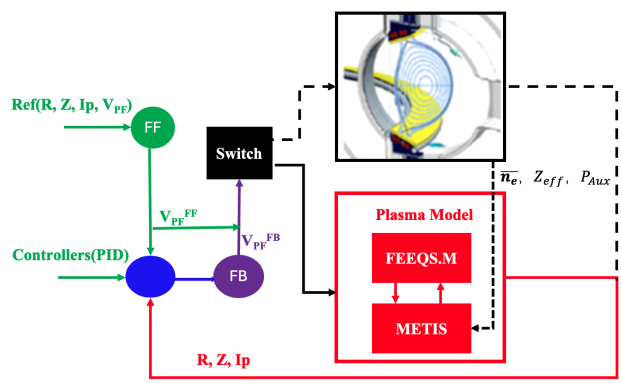


Fig. 1: Schematic of integrated workflow

The integrated workflow is first used to verify #3293 with a VDE in the HL-3. This shot aims to achieve a target $I_p \sim 1.5\ MA$ with $\kappa \sim 1.5$. Due to the limited flux swing provided by the CS coil, the plasma shape has to transition from limiter to divertor, meaning $\kappa$ increases from 1.0 to 1.5 as $I_p$ ramps up. This dynamic scenario introduces significant oscillations, e.g., $j_\phi$ evolves drastically in response to changes $\beta_p$ and $l_i$. These rapid variations are associated with fast modifications in $R$, $Z$ and $I_p$, pushing the $FF+FB$ control loop into an intensive working state, with $V_{PFs}$ as the only available actuators. Ultimately, this highly dynamic shot ends in a VDE-induced disruption. The verification between simulation and experimental data is presented in Fig. 2. At the beginning of the simulation, the plasma boundary is forced to match the magnetics-constrained EFIT reconstruction. As the simulation progresses, the plasma boundary deviates from the EFIT reconstruction, particularly during the transition from limiter to divertor. This discrepancy arises because the FB strategy regulates $R,Z$ rather than iso-flux or gap-based approach. However, the boundary remains close to EFIT due to the influence of robust $V_{PF}^{FF}$. Nevertheless, the well-matched $R,Z$ and $I_p$ on the right of Fig. 2, suggesting a strong verification of the experiment by the developed model. The overlapping $\beta_p$ and $l_i$ between FEEQS.M and METIS further demonstrate consistency between equilibrium and transport simulations. Finally, the similarity of $I_{vv}$ compared to experimental data indicates that a reliable model for vacuum vessel has been employed in FEEQS.M.

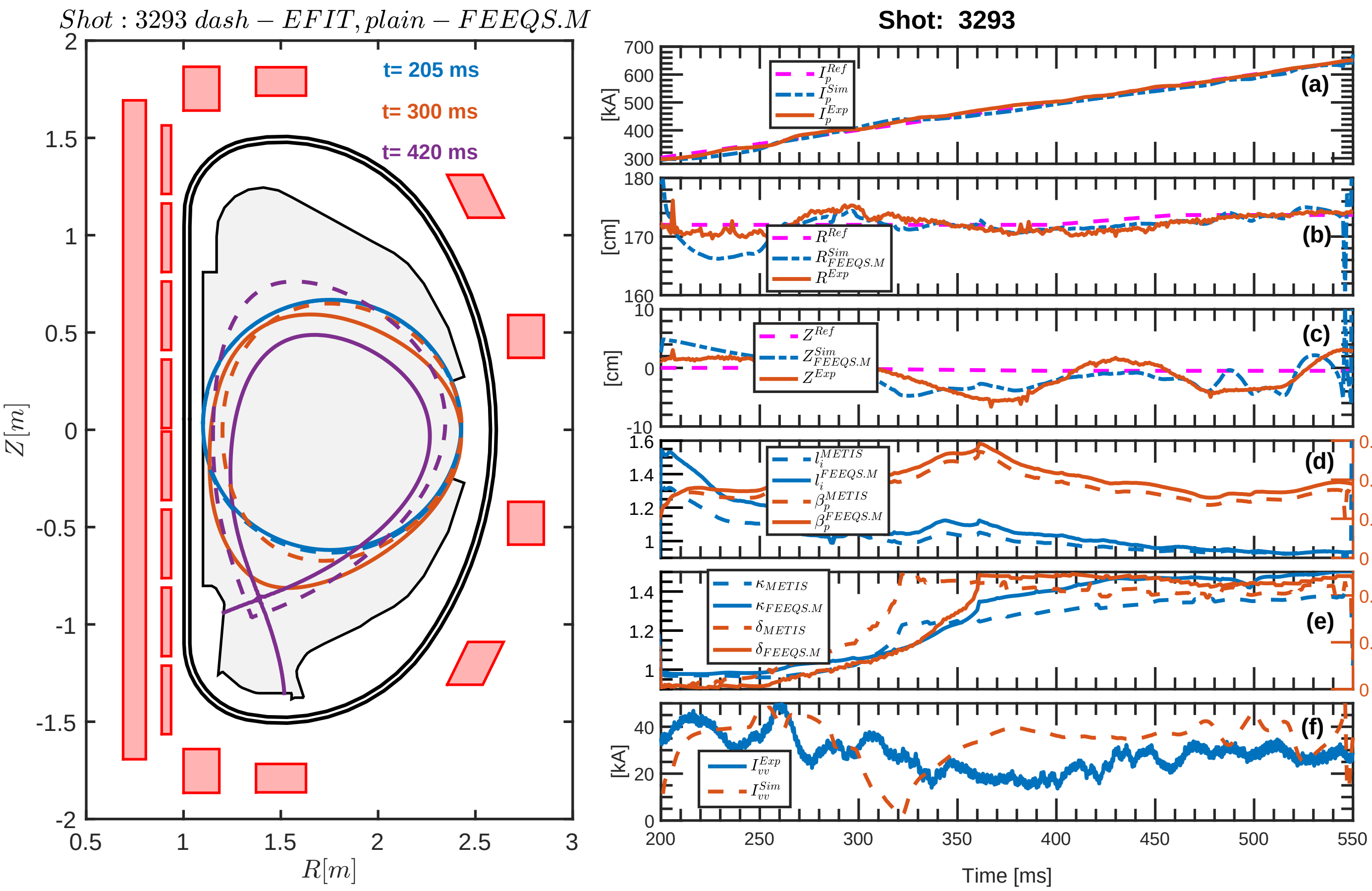


Fig. 2: Comparison between simulation and experiment. Left: Plasma boundary from FEEQS.M (plain) and EFIT (dash) at different time steps. Right: (**a**) $I_p$, (**b**) $R$, and (**c**) $Z$ from experiment (plain) and FEEQS.M (dash); (**d**) $\beta_p$ and $l_i$ from FEEQS.M (plain) and METIS (dash); (**e**) $\kappa$ and $\delta$ from FEEQS.M (plain) and EFIT (dash); (**f**) eddy currents in vacuum vessel from FEEQS.M (dash) and experiment (plain).

With the aforementioned verification, the workflow is then applied to optimize the nominal shot to avoid VDE-induced disruptions. It is found that, using the experimental controller gains with optimization for $R^{Ref}$, the dynamic scenario remains a smooth shape transition and $j_\phi$ diffusion. As an alternate approach, deploying advanced control strategies, such as iso-flux and gap control, to replace simple $RZI_p$ loop can also lead to an optimized scenario for VDE avoidance.

This work has been partly supported by the National MCF Energy R&D Program of China under Award 2019YFE03040002, and by the CNNC Science Fund for Talent Young Scholar under Award 2022JZYF-01.

[1] LAZARUS, E., LISTER, J., and NEILSON, G., Nucl. Fusion **30** (1990) 111.
[2] SONG, X., LI, B., ZHOU, J., et al., Nucl. Fusion **61** (2021) 086010.
[3] BLUM, J., HEUMANN, H., NARDON, E., and SONG, X., J. of Comput. Phys. **394** (2019) 594.
[4] ARTAUD, J.-F., IMBEAUX, F., GARCIA, J., et al., Nucl. Fusion **58** (2018) 105001.